ACS OMEGA

Open Access

http://pubs.acs.org/journal/acsodf

Article

Chitosan-Cement Composite Mortars: Exploring Interactions, Structural Evolution, Environmental Footprint and Mechanical Performance

Haci Baykara,* Ariel Riofrio, Natividad Garcia-Troncoso, Mauricio Cornejo,¶ Ken Tello-Ayala,¶ Jorge Flores Rada,¶ and Julio Caceres¶

Cite This: *ACS Omega* 2024, 9, 24978−24986

Read Online

ACCESS | Metrics & More | Article Recommendations | Supporting Information

ABSTRACT: The increasing environmental concerns about synthetic polymers as reinforcement in the construction industry have highlighted the need for eco-friendly, biodegradable fibers as potential alternative materials for cementitious composites. This study examines the influence of chitosan particle concentrations on the midterm compressive strength of mortars. Chitosan particles, derived from shrimp shells, were mixed with high early strength hydraulic cement at various percentages (0, 0.05, 0.25, 0.5, 1, and 2 wt %) and silica sand to prepare the mortar samples. The findings indicate that chitosan affects the hydration process through the distribution of chitosan particles within the mortar matrix and slightly improved midterm mechanical properties. A life cycle assessment (LCA) revealed a slight increase in greenhouse gas emissions and embodied energy for chitosan-modified mortars, likely due to the use of chemicals in the chitosan synthesis and purification process. In fact, the addition of 0.25 wt % of chitosan into the mortar only added 1.3% of the global warming potential of the sample when compared to the control sample. Incorporating chitosan into a mortar matrix does not significantly affect the resistance-mechanical properties of the composite. The hydration of the cement mortar appears to be slowed by the inclusion of chitosan particles in the cementitious matrix. This research lays the groundwork as one of the first studies for the development of high-performance, early strength cement using chitosan, contributing to a more sustainable construction industry.

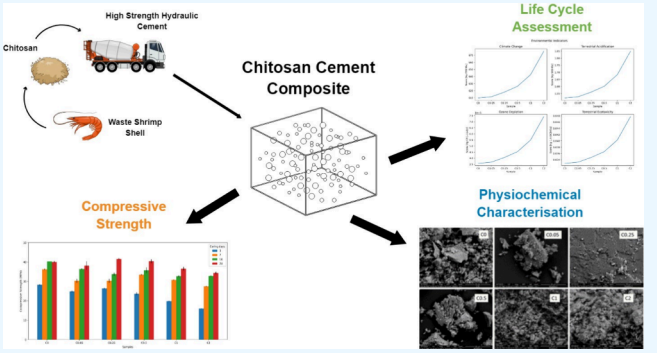

1. INTRODUCTION

Cement mortars, concrete, and different mixtures based on Ordinary Portland Cement (OPC) are the most commonly used construction materials in society because of their low cost, high strength at short application times, and durability.[1] The demand for cementitious materials continues to grow as society advances in developing countries. However, there are still several issues with concrete that require further research to focus on the self-healing of concrete or reducing its environmental impact. Another issue faced by cement is that it corresponds to a quasi-brittle material that usually has a low tensile strength resistance.[2] Under stress, this might result in cracking of the cement, which causes significant stability, load resistance capacity, safety risks, and economic burdens related to the cement structure.[3] These problems tend to be disregarded as the main focus lies in the immediate behavior of the cement mortar, while less analysis is performed on the long-term effect on the properties and environmental impact of the cement or concrete.[4]

The main goal of cement research is to modify the resistance and durability of cement, which will have a significant impact on economics and sustainability. A more durable cement or concrete requires less maintenance, has a longer life, and reduces the carbon footprint in the long term. The use of natural or synthetic polymeric materials as reinforcements in cement has been studied to improve its properties, such as a tensile strength.[3] Polymers are of great value as an effective option for changing the behavior of cement. Some studies have indicated that the use of polymers in cement mortar has a positive impact on water penetration and corrosion by chemicals.[5,6] Nonetheless, the use of synthetic polymers provides a new issue in terms of environmental burden when using fiber reinforcement at high volumes of concrete, as the market requires.

Chitin is one of the most abundant biopolymers naturally occurring in nature, second only to cellulose. Normally, chitin

Received: March 1, 2024
Revised: April 30, 2024
Accepted: May 10, 2024
Published: May 30, 2024

can be extracted from the exoskeletons of different living organisms, such as fungi,[7] insects,[8] and crustaceans.[9] Chitosan, which is obtained from chitin, has some unique properties that are interesting for its use as a composite, such as biocompatibility, antimicrobial activity, and biodegradability.[10] However, only a few studies have evaluated the effects of biopolymers on the mechanical properties of OPC mortars.[11−13] Chitosan and char chitosan have been used in cement composites, with evidence showing an incipient fracture toughness capability.[14] Another study on modified chitosan showed that an increase in chitosan content delayed the dissolution of alite, prolonged the hydration process, and transformed capillary pores into gel pores.[15] Moreover, chitosan has been modified to act as a superplasticizer, and the results showed better performance in terms of the retarding effect and compressive strength.[16]

This study analyzed the compressive strength of chitosan as a binding aggregate in the cement matrix at different low dosages of biopolymers. Moreover, characterization techniques were applied to assess the different interactions between chitosan and cement material from a chemical binding perspective. Through spectroscopy, X-ray diffraction, thermal stability analysis, and morphological characterization, this study aims to establish a comprehensive link between chitosan dosage, compressive resistance, and various material properties. In addition, the environmental profile of the cement mixtures was evaluated through life cycle assessment to provide a complete approach for the development of sustainable materials.

2. EXPERIMENTAL SECTION

High-initial-strength hydraulic cement, commercially known as HOLCIM PREMIUM HE, was obtained from Holcim S.A. Ottawa 20−30 sand was used.[17] Chitosan was produced from dried shrimp shells obtained from Santa Priscila S. A., Ecuador. NaOH (reagent grade, ≥ 98%, anhydrous pellets) from Merck and HCl (ACS reagent, 37%) were purchased from Sigma-Aldrich. The cement complied with the technical specifications shown in Table 1.

Table 1. Cement HE[a] Properties

Physical Properties	Value
Length change per autoclave	−0.02%
Setting time, Vicat's method[18]	130 min
Air content in the mortar, by volume	5%
Curing Day	Compressive Strength
1	14 MPa
3	27 MPa
7	34 MPa
28	42 MPa
Expansion in mortar bars 14 days	0.002%

[a]HE cement follows the ASTM C1157 standard[19]

Chitosan was prepared using the following detailed elsewhere.[20] In brief, shrimp shells were cleaned using tap water to get rid of larger particles, and excess meat. Then, the shells were exposed to a solution of NaOH (3 wt %, 1:10 shell: solution) to remove the remaining proteins, at 65 °C for 2h. Afterward, the deproteinated shells were immersed into a demineralization process using HCl (1N, 1:15) at room temperature for 6h. Finally, isolated chitin was deacetylated using NaOH at 100C for 5 h. Additional, decolorization H2O2 was performed to remove the pigments and remaining impurities.[20] The average deacetylation percentage of the chitosan particles is approximately 85%[21] based on the peaks shown in Figure 1 at different wavelengths.

Mix Proportions and Specimen Preparation. Cement and chitosan were mixed into different composite samples. Table 2 provides a detailed overview of the six dosage combinations consisting of HE cement, 20−30 Ottawa sand, water, and chitosan.

Tests were performed by subjecting the specimens to compression loads at 3, 7, 14, and 28 d of resistance. Two mortar samples were prepared for each established dosage. The methodology followed was in accordance with ASTM standards.[22,23]

Compressive Strength Test. Two specimens per sample or dosage were tested for compressive strength at 3, 7, 14, and 28 d. These specimens were placed in an ELE International 2000 kN hydraulic press to ensure that they were aligned with the axes of the equipment. The press applies a compressive force until the specimen reaches its breaking point, indicating the maximum force it can withstand.

Fourier-Transform Infrared Spectroscopy (FTIR). The infrared spectra of the samples were obtained using a PerkinElmer Spectrum 100 spectrophotometer. A KBr pellet with each composite sample was prepared, and its spectra from 4000 to 400 cm^{-1} was obtained to analyze their characteristic functional groups.

X-ray Diffractometry (XRD). Crystalline structures were determined using a PANalytical model X' Pert X-ray Diffractometer. Powdered samples were mixed with ZnO internal standards for quantification. The equipment was operated under the following conditions: 45 kV, 40 mA, scanning range from to 5−80 (°2theta) with a step of 0.01°/s. A copper X-ray tube and a X' Celetor detector were used along aside with HighScore Plus software for quantification of crystalline phases.

Thermogravimetric Behavior. The thermal curves and stabilities of the composite samples were determined using a TA Instruments Q-600 instrument with simultaneous differential scanning calorimetry (DSC). The operating conditions were a nitrogen purge flow of 100 mL/min, with a step of 20 °C/min for the heating ramp in the range of room temperature to 1000 °C.

Scanning Electron Microscopy (SEM). The morphology of the samples was observed using the FEI Inspect S model under the following operating conditions: HV of 12.50 kV, BSED detector, and spot size of 3.5. Different magnifications were collected from 500 to 10000x.

Environmental Modeling. The environmental impact assessment was conducted in accordance with ISO 14040[24] regulation for life cycle assessment (LCA). The system was modeled from a cradle-to-gate perspective, with a focus on the impact of the materials used in the cement composite. The functional unit for the system was set as 3130 kg of cement composite, which was equivalent to 1 m^3 of cement composite mortar.

The chitosan particles were modeled based on the findings of Riofrio et al.[9] with some modifications to the amount of NaOH and HCl used. The reuse of solutions for deproteinization, demineralization, and deacetylation was set at four times before new solutions were prepared and used based on experimental data. The cement HE used in the composite and its background data were taken from Petroche et al.,[25] who

https://doi.org/10.1021/acsomega.4c02040
ACS Omega 2024, 9, 24978−24986

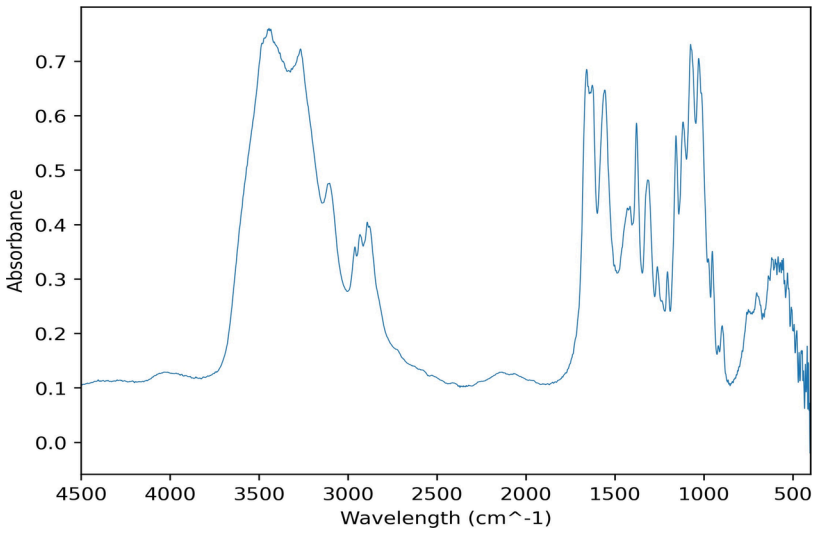

Figure 1. FTIR spectroscopy of chitosan was used as a reinforcement material.

Table 2. Mortar Proportions

Sample #	Code	HE Cement (g)	Sand20−30(g)	Water (g)	Other (g)	Fluidity (%)	Chitosan (%)
Control sample	C0	740.00	2035	355	0.00	114	0.00
2	C0.05	739.63	2035	355	0.37	109	0.05
3	C0.25	738.15	2035	355	1.85	110	0.25
4	C0.5	736.30	2035	355	3.70	114	0.50
5	C1	732.60	2035	355	7.40	110	1.00
6	C2	725.20	2035	355	14.80	109	2.00

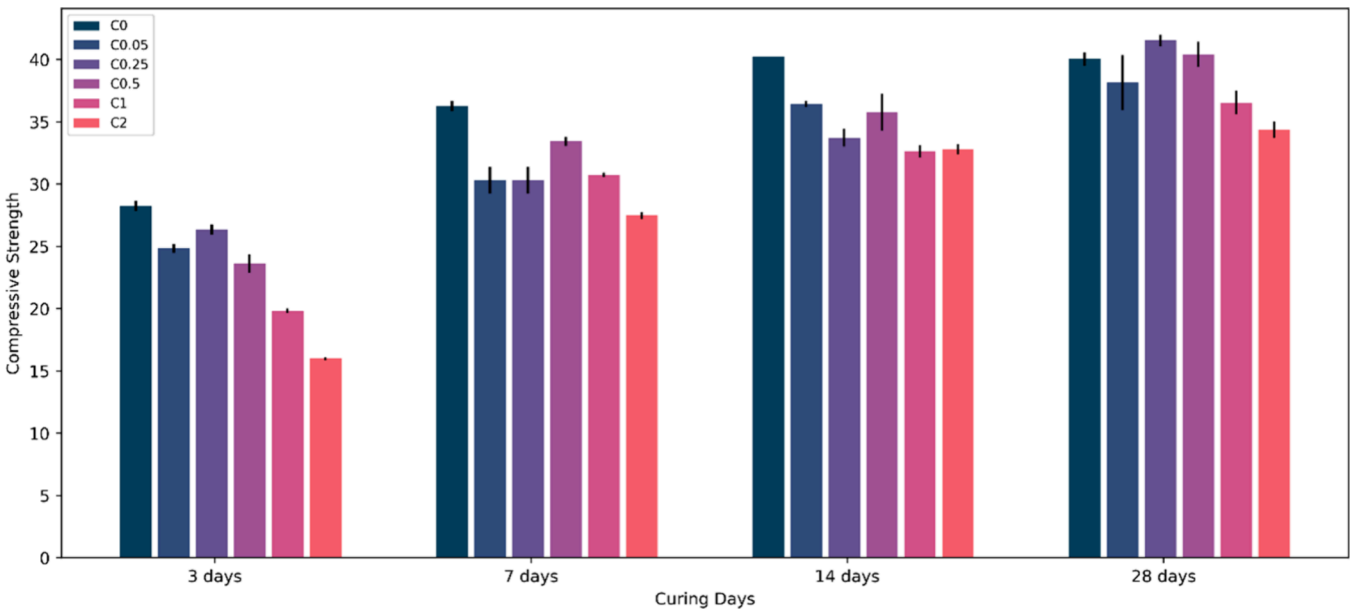

Figure 2. Comparison of compressive strengths (MPa) of samples at different times.

elaborated the profile of clinker and cement from Ecuador. The silica sand was modeled using the available inventory from Ecoinvent 3.7.[26] All inventory data inputted into OpenLCA software were converted to an impact indicator using ReCiPe Midpoint H.[27] The six samples were analyzed under four impact indicators of interest for construction materials:[28] climate change, terrestrial acidification, ozone depletion, and terrestrial ecotoxicity.

3. RESULTS AND DISCUSSION

The compressive strengths of samples C0.025 and C0.5 were better than those of plain concrete at 28 d. However, at short curing times, concrete still outperformed the behavior of the chitosan-cement composite. This might be related to the water-binding properties of chitosan, which may cause the concrete composite to cure slowly. As shown in Figure 2, the samples that included chitosan in their composition showed a decrease in their resistance compared to the control sample.

https://doi.org/10.1021/acsomega.4c02040
ACS Omega 2024, 9, 24978−24986

The samples with the greatest decrease in resistance were C2 and C1, with 37% and 23%, respectively, after 3 days of curing. In contrast, sample C0.025, which contained 0.025% chitosan, presented a 4% increase in resistance at 28 days compared to the standard sample. This behavior reinforces the importance of analyzing cement matrices not only by their rapid compressive resistance but also by the long-term performance of such materials.

The cement with no chitosan in its composition (C0) reached its maximum strength at 14 days, and it seemed to maintain a compressive strength of approximately 40 MPa after 14 days of curing. In contrast, the samples containing chitosan appeared to continue to become tougher as the curing time increased (Figure 2). At 3 days, the compressive strength of the samples decreased with the addition of chitosan to the mortar. However, C0.25 and C0.5, at 28 days, exempt the behavior explained. At 28 days, C0.25 performs slightly better than the regular cement mortar, statistically may not appear as a difference, but at least performs equally to C0. This may be due to the better dispersion of chitosan in the cement mortar, which allows for a reduction in the total pore volume. Based on the narrow standard deviation of the mechanical strength in the samples we can infer that chitosan particles have indeed dispersed well in the mortar composites. This finding aligns with a study that concluded that the use of chitosan at 1% w/w concentration in cement mortar had a positive impact on the distribution, total pore volume, frost resistance, and biostability of the composite.[12]

Vysvaril et al.[13] analyzed the effects of different chitosan ethers on lime mortar. Mortars containing more than 1% chitosan ethers showed higher water retention and mortar thickening. This phenomenon explains why C1 and C2 show lower compressive strength even at 28 days, as the curing process takes up more time because of the water retention occurring because of the inclusion of chitosan in the composition. Other properties of the cement added to the mortar should be reviewed owing to the use of chitosan. A series of studies evaluated the incorporation of modified chitosan into a cement matrix. Chitosan showed a higher water retention.,[29] at least 10% more retention for less than 1% chitosan added. On the other hand, chitosan with different molecular weights and its impact on thickening and retaining heavy metals have been also reported.[11] The study showed that the use of chitosan, regardless of the molecular weight of chitosan, resulted in an average increase of 3% in water retention. Additionally, the increase in viscosity at higher compositions (1:3 binder to chitosan composition) may be attributed to entanglement between the polymer chains precipitated in an alkaline or calcium-enriched environment.[11,30] The thickening effect of chitosan in a calcium-rich environment increases due to greater entanglement and cross-linking between the polymer chains and the calcium ions in the cement. While the setting time at low chitosan dosages is primarily affected by the degree of deacetylation, it becomes the dominant factor at higher dosages. Chitosan has also been reported to delay the setting of cement mortars.[31] Chitosan can have a potential binding effect (as represented in Figure 3) with cement particles, forming complexes with Ca^{2+} ions as suggested in the literature.[32,33]

FTIR. The FTIR spectra of the sample that exhibited good performance after 28 days (C0.25) are shown in Figure 4. Several peaks were observed at 3, 7, 14, and 28 d, which were repeated throughout the samples. The broad peaks at 3400 and

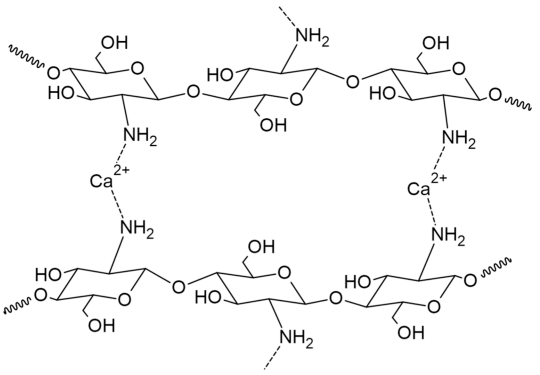

Figure 3. Representation of the complexes may form between calcium ions in the cement and especially amino groups in the chitosan biopolymer.

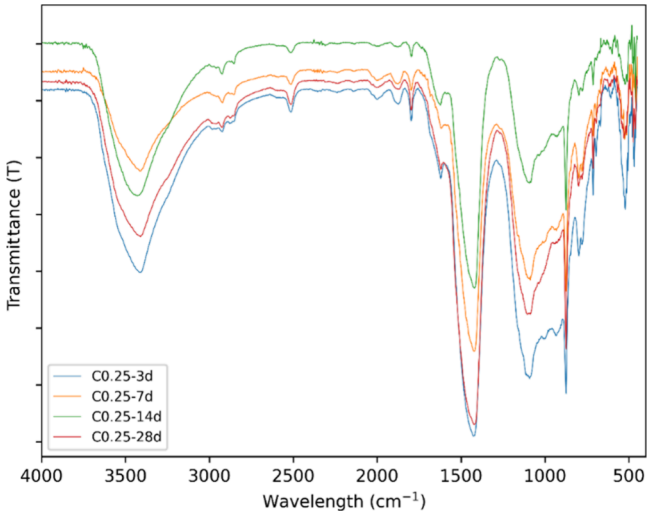

Figure 4. Infrared spectra for sample C0.25 at curing days 3, 7, 14, and 28.

1620 cm^{-1} were attributed to the stretching of −OH from the portlandite or calcium hydroxide component and -NH from chitosan. The high absorbance peaks around 1420 and 870 cm^{-1} correspond to carbonate ions. Around 1100 cm^{-1} is the peak for the interaction of the S−O bond.[34,35] The C−H bond was observed at 2926 cm^{-1}. Several peaks are related to carbonate ions originating from calcium or magnesium. A peak around 1559 cm^{-1} that is linked to chitosan is not observed in the FTIR graph because of the low percentage used in the cement matrix.[36] In the Supporting Information File in Figures S1−S4 the spectra of the samples cured for 3, 7, 14, and 28 days are shown.

XRD. The cement has some characteristic peaks that can be observed through the XRD analysis. In this study, samples using silica sand and high-strength cement were analyzed at 3, 7, 14, and 28 days (Figure S5−S8 in the Supporting Information File). The analysis showed that quartz peaks were found in approximately 24, 31, and 71°2theta (Figure 5). Two peaks found at 34°and 67° correspond to calcium silicate hydrate (CSH), and two peaks are linked to calcium silicate in the form of C2S at 37−38 and 56°. Figure S5−S8 shows each sample on each analyzed day, as mentioned earlier. Across every sample, the peaks were discussed, with intensity depending on the curing time. This may also be an overlay of different components in the analysis. However, this

https://doi.org/10.1021/acsomega.4c02040
ACS Omega 2024, 9, 24978−24986

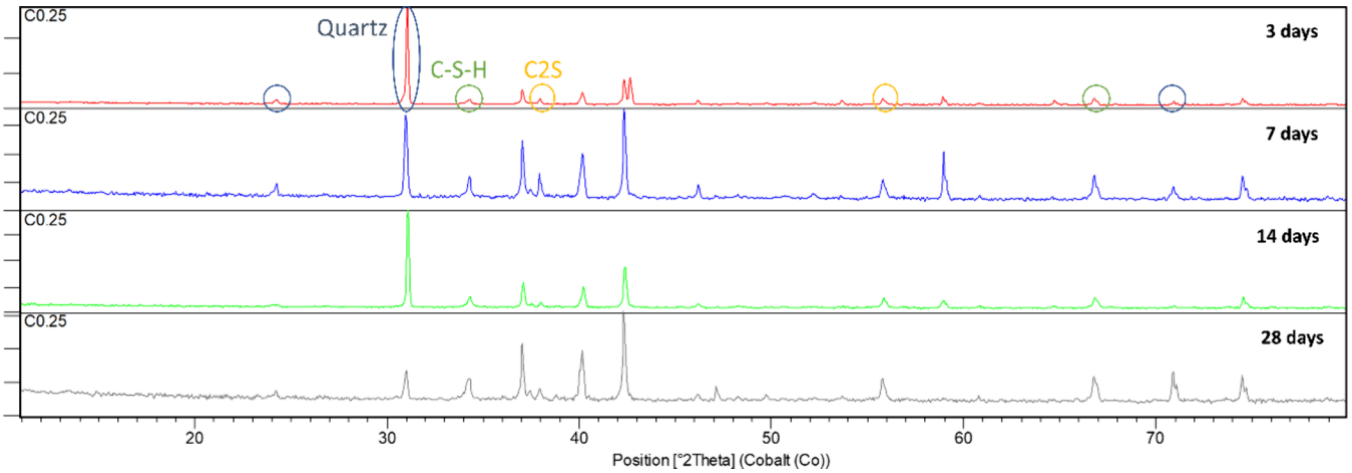

Figure 5. X-ray diffraction patterns for sample C0.25 at 3, 7, 14, and 28 days.

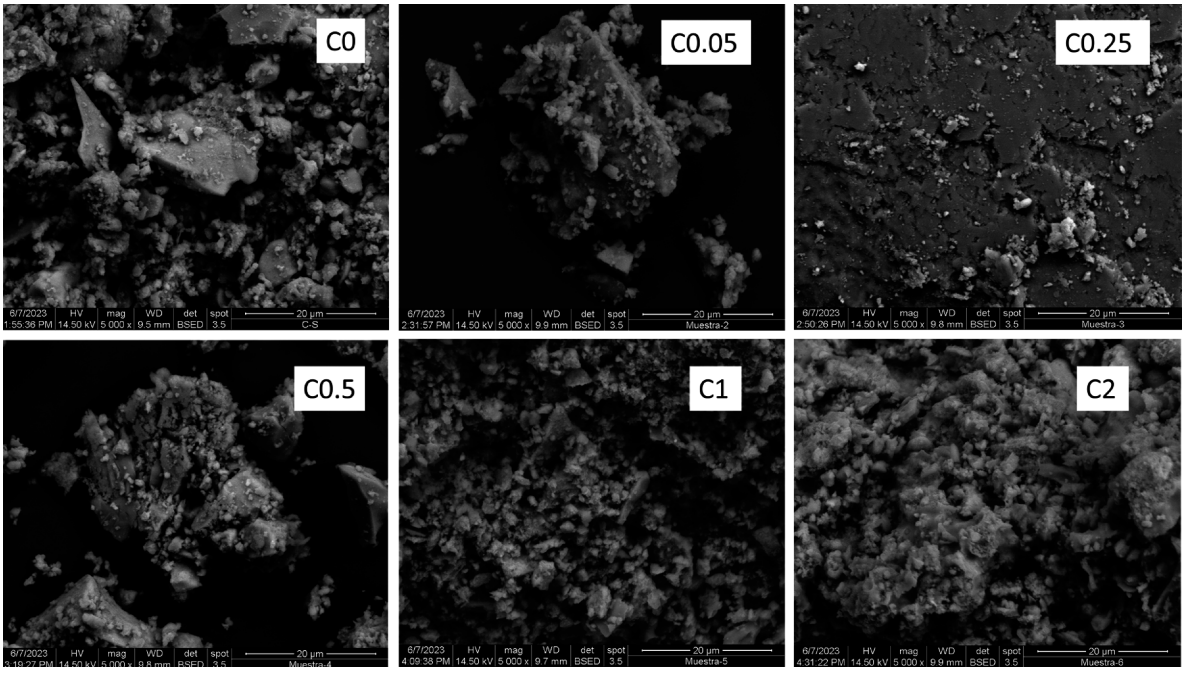

Figure 6. SEM images of samples C0, C0.05, C0.25, C0.5, C1, and C2 at 28 d of curing and at magnification of 5000×.

tendency indicates that the intensity of quartz and other components is reduced when curing advances. In addition, the quantitative results for samples C0 and C0.25 (Figure S9 and S10 in the Supporting Information File, respectively) showed a significant decrease in quartz and an increase in the amorphous content.

Thermogravimetric Analysis. The thermogravimetric analysis for sample C0.25 shows four significant mass drops in the analyzed range from RT to 1000 °C. The weight loss in the first zone corresponds to the water molecules found in the cement composite. After 28 d of curing, most of the water was lost in the process or found its way into a more stabilized structure within the composite. The cement under thermogravimetric analysis has three main zones of assessment. The first zone corresponds to the water, as mentioned earlier, evaporating from the surface or in the sample but not bonded (25−105 °C), and the decomposition of hydrates (105−400°). Then, the cement was dihydroxylated in the range of 400−600 °C, and finally, calcium carbonate (600−800 °C). The limit of free water in the 100−140 °C varies depending on the author,[37,38] in our study, we observed one peak at approximately 120°, which corresponds to free water in the cement mixture. Based on the method proposed by Bhatt,[39] which calculates the degree of hydration using the three zones previously mentioned, the C0.25 sample at 28 days presents a degree of hydration of 17.56%, which corresponds to approximately 4.2 wt % of chemically bound water in the sample. The C0 sample at 28 d had a degree of 10.26% (~2.5 wt.%), TGA/DTA curves for all samples can be seen on Figure S11 in the Supporting Information File. More water reacted with the cement paste when 0.25% chitosan was added, which corresponds with the slight increase in compressive strength. Therefore, chitosan can be used as an additive to aid the hydraulic reaction, causing the cementitious material to form higher percentages of C−S−H.[37] However, an increase in hydration can be seen in pozzolanic materials that contain alumino-silicates, such as fly ash.[40]

https://doi.org/10.1021/acsomega.4c02040
ACS Omega 2024, 9, 24978−24986

Scanning Electron Microscopy (SEM). The surfaces of the control sample and the cement-chitosan composites and their morphologies are shown in Figure 6. The composites were ground into powder and analyzed to observe the surface of each sample. More irregularities were found as the chitosan content increased, which might be due to the hydration process of the samples. The samples are in order from top to bottom and left to right as C0, C0.05, C0.25, C0.5, C1, and C2.

Samples C0 and C0.25 were collected from the compressive strength test and observed under a microscope (see figure S12 in the Supporting Information File). At 28 days, the porosity of the cement composite was reduced because of hardening related to the hydration of the cement.[41] Irregularities that might be linked to the high quartz content of the sand and the cement itself in the samples can be seen.[42] Figure 6 shows the SEM images of both samples; sample C0.25 (B) shows more surface irregularities in the cement, with what appears to be hexagonal shapes related to the cement (1000x and 2500x), whereas C0 (A) shows a smoother surface (2500x). This can be explained by the hydration of C0, which may have reached its final stage;[41] in contrast, C.25 can still suffer some hardening. In addition, particles in the white shade on sample C0.25 appeared in different parts of the sample analyzed by SEM, which might be due to the chitosan used as an additive; however, EDS should be used to positively identify these spots as chitosan. This morphology reaffirms that the hydration of cement when 0.25% chitosan is used in the cement matrix is slower than that of pure cement.

Statistical Significance. An F-value of 0.019 revealed a minor difference between the groups at 3 days after rupture (see Table 3). On the day of rupture, a p-value of 0.892 indicated that no statistically significant difference was found in the compressive strengths across different samples. Consequently, we were unable to reject the null hypothesis, which suggests that the compressive strengths were comparable.

Table 3. Analysis of Variance for Chitosan-Geopolymer Composites

	Curing days				
ANOVA Test Parameter	3	7	14	28	Overall
F-value	0.019	0.311	0.099	1.509	0.057
P-values	0.892	0.589	0.759	0.247	0.812

Seven days after rupture, an F-value of 0.311 indicates moderate variance across groups. On this rupture day, the p-value of 0.589 suggests similar findings as before, with no significant difference. Consequently, we failed to reject the null hypothesis, implying that the compressive strengths were comparable.

An F-value of 0.099 indicates a minor difference between the groups 14 days after rupture. On this rupture day, the p-value of 0.759 suggested that there was no statistically significant difference. Consequently, we were unable to reject the null hypothesis; thus, the compressive strengths were similar.

At 28 days after rupture, an F-value of 1.509 indicated moderate variance between the groups. On this rupture day, a p-value of 0.247 indicates that there was no statistically significant difference in compressive strength across the groups. Consequently, we were unable to reject the null hypothesis, indicating that the compressive strengths were comparable.

The F-value for the overall ANOVA findings was 0.057, indicating a minimal overall variation between the groups. A p-value of 0.812 indicates that there was no statistically significant difference in the compressive strengths across the groups. Consequently, we were unable to reject the null hypothesis, which means that the compressive strengths were comparable.

In summary, based on the ANOVA results for each rupture day and the overall analysis, there was no significant difference in the compressive strengths among the different samples on any of the rupture days or overall.

Life Cycle Assessment. The use of chitosan in the cement matrix is expected to increase the global warming potential of cement composites, as 1 kg of chitosan approximately produces 5−6 kg of CO_2 eq For this reason, in Figure 7, we see a behavior of adding a climate change score when chitosan is added at a higher percentage. However, if we consider the C0.25 sample that had a slightly better performance at 28 days, the climate change score from C0 and C0.25 was only ∼1.3% higher for the latter. The literature shows that for 1 ton of hydraulic cement, the climate change score ranges from to 632−950 kg of CO_2 eq,[25] with an average for different types of cement of 693 kg of CO_2 eq[43] In this study, a maximum of 0.74 tons of hydraulic cement HE was used, and the rest was added silica sand; thus, we found similar values to those found in the literature with the inclusion of chitosan. The EcoInvent Data set[44] indicates that 1 kg of polypropylene or polyethylene terephthalate inventory has an additional carbon footprint of 3 and 2 kg of CO_2 eq In comparison, Chitosan exhibits a 66% and 150% higher environmental impact, respectively. However, it is important to note that a crucial factor has not been considered, namely, the prevention of waste (shrimp shell) from being disposed of in a landfill. The substantial greenhouse gas emissions per ton of waste sent to a landfill have already been evaluated, with estimates ranging from several hundred to thousands of kg of CO_2 emitted.[45,46] In fact, avoiding the disposal of 35 kg of waste in the municipal solid waste treatment process can have a significant impact on the climate change category by lowering the impact to a negative indicator. This suggests that the biopolymer captures carbon instead of producing CO_2 emissions. While shrimp shell is typically processed into animal feed, thereby excluding the landfill scenario as the primary scenario, it is essential to acknowledge the use of waste that reduces the environmental burden of the biopolymer.

One study[47] that assessed the impact of different fibers on the flexural strength of cement also evaluated the environmental performance of different mixes. The cement matrix with virgin carbon fibers (vCF) has the highest results with 739 kg CO_2 eq, the glass and poly(vinyl alcohol) fiber cement composite were ∼120% higher than the reference cement matrix.[47] In contrast, our highest score (670 kg CO_2 eq) was only ∼10% higher than the reference (G0). Another study[48] that evaluated the performance of concrete that included PVA fiber (1.0−1.7%), recycled concrete particles (15−45%), and fly ash resulted in 16 mixtures that fluctuated around 600 kg CO_2 eq for the climate change indicator, with the optimal mixture exceeding 400 kg CO_2 eq Similar results were found for the evaluated mortars in this study with values from ∼610−670 kg CO_2 eq depending on the concentration of chitosan, and the addition of coarse aggregates to a concrete mixture can

https://doi.org/10.1021/acsomega.4c02040
ACS Omega 2024, 9, 24978−24986

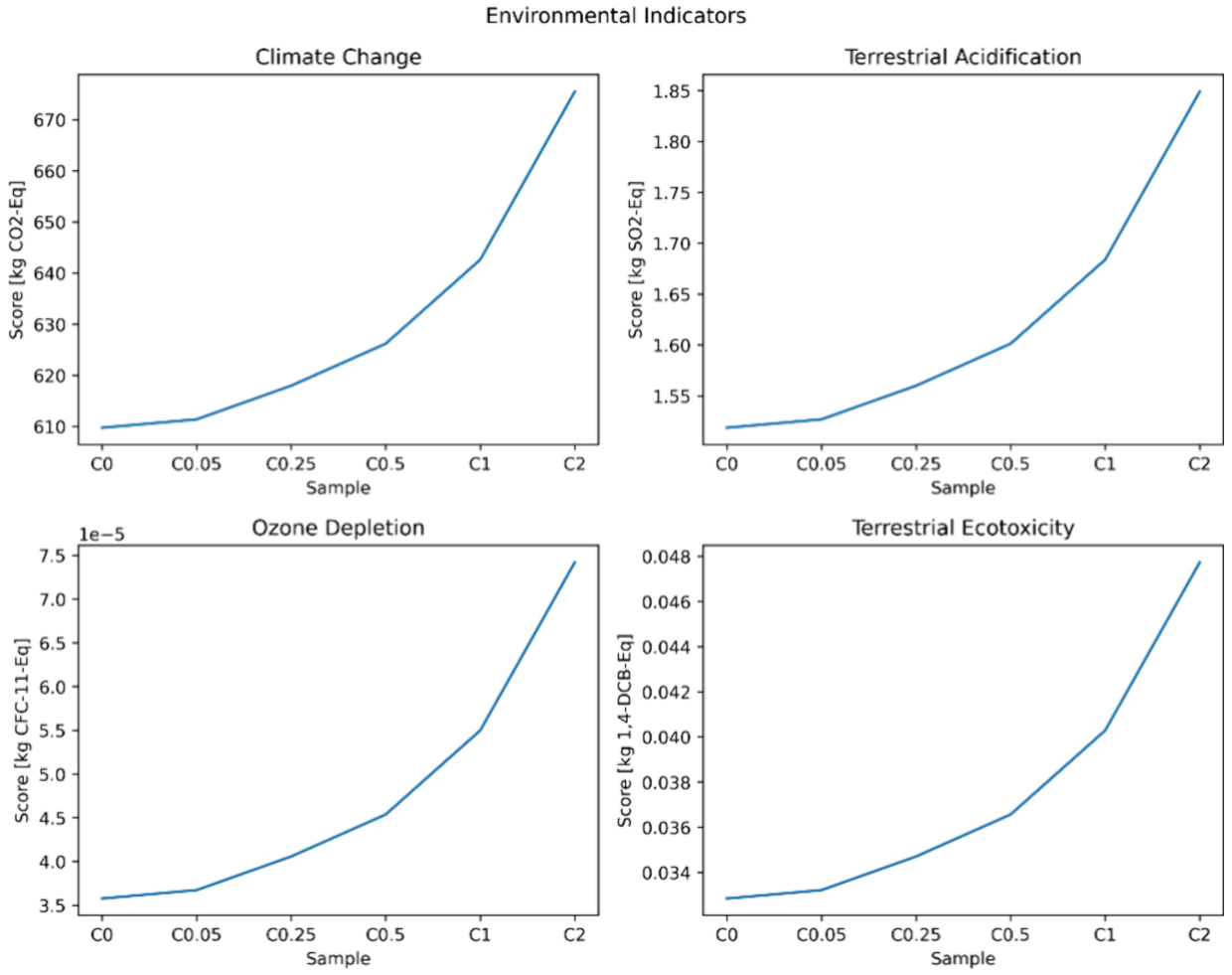

Figure 7. Environmental indicators for the chitosan-cement mixtures using ReCiPe Midpoint H.

drastically lower the results to 400 kg CO_2 eq for the climate change parameter.

A similar tendency was observed for the other environmental impact categories. The control sample for terrestrial acidification (TA) had a score of 1.52 kg SO_2 eq with a difference of 21.7% increase for C2. The fibers in the study conducted by Akbar et al.[47] had a reference of 1.33 kg SO_2 eq; however, the fibers had an increase of up to 225% (~3 kg SO_2 eq for virgin carbon fiber). In fact, when the fiber was included in 2% volume, the TA increases to 4.5 kg SO_2 eq In the ozone depletion category, our study has 10 times more environmental burden compared to the literature,[43,47] which is related to the fiber and its upstream processes. The evaluated cement mortars in this study showed improvement in most cases when compared to the average European cement production of different types, such as CEM I, II, III, IV, and V.[43]

4. CONCLUSIONS

This research highlights the potential of chitosan as an environmentally friendly reinforcement material for concrete. The interaction between chitosan and high initial strength cement was studied for five different chitosan-cement composites and a control sample. The resistance to mechanical forces (compressive strength) for six samples and the characterization of functional groups, thermal degradation, crystalline structure, and morphology were evaluated for the control sample and the highest-scoring composite sample at 28 days.

At short curing periods, chitosan cement composites exhibited lower compressive strengths. However, at 28 days, cement containing 0.25 and 0.5% chitosan in the cement matrix, showed a slight increase in compressive strength. Results show that cement that incorporates chitosan is not affected by its resistance-mechanical properties in the long run. The hydration of the cement mortar appears to be slowed by the inclusion of chitosan particles in the cementitious matrix.

Despite an anticipated increase in the global warming potential, the climate change score for C0.25, with slightly better performance at 28 days, was only ~1.3% higher compared to C0. This marginal difference aligns with comparable values found in the literature for conventional cement production. The study underscores chitosan's viability for sustainable construction, as its environmental impact remains competitive with alternative materials, such as virgin carbon fibers and PVA fiber. Crucially, the incorporation of chitosan into cement does not compromise long-term mechanical properties.

Additional investigation is necessary to comprehensively understand the impact of chitosan on the mechanical properties and endurance of concrete. Future studies should examine the influence of chitosan on other mechanical properties, such as flexural strength, tensile strength, and modulus of elasticity. Moreover, the durability aspects of

https://doi.org/10.1021/acsomega.4c02040
ACS Omega 2024, 9, 24978−24986

chitosan-enhanced concrete, including its resistance to corrosion, freeze−thaw cycles, and other environmental degradation mechanisms, should be explored. By pursuing these research avenues, we can gain a more profound understanding of the potential of chitosan-enhanced mortar as a sustainable and durable construction material.

■ ASSOCIATED CONTENT

Supporting Information

The Supporting Information is available free of charge at https://pubs.acs.org/doi/10.1021/acsomega.4c02040.

FTIR spectra, Quantitative XRD, TGA curves, and SEM images of the cement samples at different curing days (PDF)

■ AUTHOR INFORMATION

Corresponding Author

Haci Baykara − *Facultad de Ingeniería Mecánica y Ciencias de la Producción, Escuela Superior Politécnica del Litoral, ESPOL, Guayaquil 090112, Ecuador;* orcid.org/0000-0002-8319-0836; Email: hbaykara@espol.edu.ec

Authors

Ariel Riofrio − *Department of Civil and Environmental Engineering, The Hong Kong University of Science and Technology, Clear Water BAY, Kowloon, Hong Kong SAR; Facultad de Ciencias Naturales y Matemáticas, Escuela Superior Politécnica del Litoral, ESPOL, Guayaquil 090112, Ecuador;* orcid.org/0000-0003-3968-1176

Natividad Garcia-Troncoso − *Facultad de Ingeniería en Ciencias de la Tierra and Centro de Investigación y Desarrollo de Nanotecnología, Escuela Superior Politécnica del Litoral, ESPOL, Guayaquil 090112, Ecuador;* orcid.org/0000-0002-1630-4274

Mauricio Cornejo − *Facultad de Ingeniería Mecánica y Ciencias de la Producción, Escuela Superior Politécnica del Litoral, ESPOL, Guayaquil 090112, Ecuador; Centro de Investigación y Desarrollo de Nanotecnología, Escuela Superior Politécnica del Litoral, ESPOL, Guayaquil 090112, Ecuador*

Ken Tello-Ayala − *Facultad de Ingeniería en Ciencias de la Tierra, Escuela Superior Politécnica del Litoral, ESPOL, Guayaquil 090112, Ecuador*

Jorge Flores Rada − *Centro de Innovación Holcim, Holcim Ecuador S.A., Guayaquil 090616, Ecuador*

Julio Caceres − *Centro de Investigación y Desarrollo de Nanotecnología, Escuela Superior Politécnica del Litoral, ESPOL, Guayaquil 090112, Ecuador*

Complete contact information is available at: https://pubs.acs.org/10.1021/acsomega.4c02040

Author Contributions

¶M.C., K.T., J.F., and J.C. contributed equally. H.B.:Writing-Conceptualization, Writing- review and editing, Supervision. A.R.: Writing-original draft, Data curation, Investigation, Methodology. Writing- review and editing. N.G.: Data curation, Investigation, Writing-original draft, Supervision. M.C., K.T., J.F., J.C.: Investigation. All authors have given approval to the final version of the manuscript.

Notes

The authors declare no competing financial interest.

■ ACKNOWLEDGMENTS

We thank Luis Aguilar and Erica Jiménez, students from FICT-ESPOL, for their help in the sample preparation stage of this study. We also extend our deep appreciation to the Hong Kong University of Science and Technology for providing the software license to conduct the LCA evaluation.

■ REFERENCES

(1) Nawaz, M. A.; Qureshi, L. A.; Ali, B.; Raza, A. Mechanical, Durability and Economic Performance of Concrete Incorporating Fly Ash and Recycled Aggregates. *SN Appl. Sci.* **2020**, *2* (2), 162.

(2) Chen, X.; Yuan, J.; Dong, Q.; Zhao, X. Meso-Scale Cracking Behavior of Cement Treated Base Material. *Constr Build Mater.* **2020**, *239*, No. 117823.

(3) Zhang, X.; Du, M.; Fang, H.; Shi, M.; Zhang, C.; Wang, F. Polymer-Modified Cement Mortars: Their Enhanced Properties, Applications, Prospects, and Challenges. *Constr Build Mater.* **2021**, *299*, No. 124290.

(4) Wang, Z.; Jin, W.; Dong, Y.; Frangopol, D. M. Hierarchical Life-Cycle Design of Reinforced Concrete Structures Incorporating Durability, Economic Efficiency and Green Objectives. *Eng. Struct* **2018**, *157*, 119−131.

(5) Hou, D.; Yu, J.; Wang, P. Molecular Dynamics Modeling of the Structure, Dynamics, Energetics and Mechanical Properties of Cement-Polymer Nanocomposite. *Compos B Eng.* **2019**, *162*, 433−444.

(6) Guo, S.-Y.; Zhang, X.; Chen, J.-Z.; Mou, B.; Shang, H.-S.; Wang, P.; Zhang, L.; Ren, J. Mechanical and Interface Bonding Properties of Epoxy Resin Reinforced Portland Cement Repairing Mortar. *Constr Build Mater.* **2020**, *264*, No. 120715.

(7) Dhillon, G. S.; Kaur, S.; Brar, S. K.; Verma, M. Green Synthesis Approach: Extraction of Chitosan from Fungus Mycelia. *Crit Rev. Biotechnol* **2013**, *33* (4), 379−403.

(8) Soon, C. Y.; Tee, Y. B.; Tan, C. H.; Rosnita, A. T.; Khalina, A. Extraction and Physicochemical Characterization of Chitin and Chitosan from Zophobas Morio Larvae in Varying Sodium Hydroxide Concentration. *Int. J. Biol. Macromol.* **2018**, *108*, 135−142.

(9) Riofrio, A.; Alcivar, T.; Baykara, H. Environmental and Economic Viability of Chitosan Production in Guayas-Ecuador : A Robust Investment and Life Cycle Analysis. *ACS Omega* **2021**, *6*, 23038.

(10) Li, J.; Zhuang, S. Antibacterial Activity of Chitosan and Its Derivatives and Their Interaction Mechanism with Bacteria: Current State and Perspectives. *Eur. Polym. J.* **2020**, *138*, No. 109984.

(11) Lasheras-Zubiate, M.; Navarro-Blasco, I.; Fernández, J. M.; Alvarez, J. I. Studies on Chitosan as an Admixture for Cement-Based Materials: Assessment of Its Viscosity Enhancing Effect and Complexing Ability for Heavy Metals. *J. Appl. Polym. Sci.* **2011**, *120* (1), 242−252.

(12) Ustinova, Y. V.; Nikiforova, T. P. Cement Compositions with the Chitosan Additive. *Procedia Eng.* **2016**, *153*, 810−815.

(13) Vyšvařil, M.; Žižlavský, T. Effect of Chitosan Ethers on Fresh State Properties of Lime Mortars. *IOP Conf Ser. Mater. Sci. Eng.* **2017**, *251*, 012039.

(14) Nisticò, R.; Lavagna, L.; Versaci, D.; Ivanchenko, P.; Benzi, P. Chitosan and Its Char as Fillers in Cement-Base Composites: A Case Study. *Boletín de la Sociedad Española de Cerámica y Vidrio* **2020**, *59* (5), 186−192.

(15) Wang, L.; Ju, S.; Wang, L.; Wang, F.; Sui, S.; Yang, Z.; Liu, Z.; Chu, H.; Jiang, J. Effect of Citric Acid-Modified Chitosan on the Hydration and Microstructure of Portland Cement Paste. *J. Sustain Cem Based Mater.* **2023**, *12* (1), 83−96.

(16) Lv, S.; Liu, J.; Zhou, Q.; Huang, L.; Sun, T. Synthesis of Modified Chitosan Superplasticizer by Amidation and Sulfonation and Its Application Performance and Working Mechanism. *Ind. Eng. Chem. Res.* **2014**, *53* (10), 3908−3916.

(17) *Arena Normalizada. Requisitos Standard Specification for Standard Sand*. NTE INEN 873; Servicio Ecuatoriano de Normalización, 2017.
(18) ASTM. *Standard Test Methods for Time of Setting of Hydraulic Cement by Vicat Needle* (ASTM C191-21); ASTM International: West Conshohocken, PA, 2021.
(19) ASTM. *Standard Performance Specification for Hydraulic Cement* (ASTM C1157-03); ASTM International: West Conshohocken, PA, 2010.
(20) Said Al Hoqani, H. A.; AL-Shaqsi, N.; Hossain, M. A.; Al Sibani, M. A. Isolation and Optimization of the Method for Industrial Production of Chitin and Chitosan from Omani Shrimp Shell. *Carbohydr. Res.* **2020**, *492*, No. 108001.
(21) Czechowska-Biskup, R.; Jarosińska, D.; Rokita, B.; Ulański, P.; Rosiak, J. M. Determination of Degree of Deacetylation of Chitosan-Comparision of Methods.. *Prog. Chem. Appl. Chitin Deriv* **2012**.*XVII*5
(22) ASTM. *ASTM C109 Standard Test Method for Compressive Strength of Hydraulic Cement Mortars (Using 2-in. or [50-Mm] Cube Specimens)*; ASTM International: West Conshohocken, PA; 2020. DOI: 10.1520/C0109_C0109M-20.
(23) ASTM C192. *Standard Practice for Making and Curing Concrete Test Specimens in the Laboratory*; ASTM International: West Conshohocken, PA; 2015. DOI: 10.1520/C0192_C0192M-14.
(24) International organization for standardization. *ISO 14040: Environmental Management—Life Cycle Assessment—Principles and Framework*; **2006**.
(25) Petroche, D. M.; Ramirez, A. D. The Environmental Profile of Clinker, Cement, and Concrete: A Life Cycle Perspective Study Based on Ecuadorian Data. *Buildings* **2022**, *12* (3), 311.
(26) Wernet, G.; Bauer, C.; Steubing, B.; Reinhard, J.; Moreno-Ruiz, E.; Weidema, B. The Ecoinvent Database Version 3 (Part I): Overview and Methodology. *International Journal of Life Cycle Assessment* **2016**, *21* (9), 1218−1230.
(27) Huijbregts, M. A. J.; Steinmann, Z. J. N.et al. *ReCiPe 2016 v1.1*; National Institute for Public Health and the Environment: Bilthoven, The Netherlands, 2016.
(28) Feng, H.; Zhao, J.; Hollberg, A.; Habert, G. Where to Focus? Developing a LCA Impact Category Selection Tool for Manufacturers of Building Materials. *J. Clean Prod* **2023**, *405*, No. 136936.
(29) Lasheras-Zubiate, M.; Navarro-Blasco, I.; Álvarez, J. I.; Fernández, J. M. Interaction of Carboxymethylchitosan and Heavy Metals in Cement Media. *J. Hazard Mater.* **2011**, *194*, 223−231.
(30) Goycoolea, F. M.; Morris, E. R.; Gidley, M. J. Viscosity of Galactomannans at Alkaline and Neutral PH: Evidence of 'Hyper-entanglement' in Solution. *Carbohydr. Polym.* **1995**, *27* (1), 69−71.
(31) Lasheras-Zubiate, M.; Navarro-Blasco, I.; Fernández, J. M.; Álvarez, J. I. Effect of the Addition of Chitosan Ethers on the Fresh State Properties of Cement Mortars. *Cem Concr Compos* **2012**, *34* (8), 964−973.
(32) Liu, H.; Bu, Y.; Sanjayan, J.; Shen, Z. Effects of Chitosan Treatment on Strength and Thickening Properties of Oil Well Cement. *Constr Build Mater.* **2015**, *75*, 404−414.
(33) Yehia, S.; Ibrahim, A. M.; Ahmed, D. F. The Impact of Using Natural Waste Biopolymer Cement on the Properties of Traditional/Fibrous Concrete. *Innovative Infrastructure Solutions* **2023**, *8* (11), 287.
(34) Bhat, P. A.; Debnath, N. C. Theoretical and Experimental Study of Structures and Properties of Cement Paste: The Nano-structural Aspects of C−S−H. *J. Phys. Chem. Solids* **2011**, *72* (8), 920−933.
(35) Shi, T.; Gao, Y.; Corr, D. J.; Shah, S. P. FTIR Study on Early-Age Hydration of Carbon Nanotubes-Modified Cement-Based Materials. *Advances in Cement Research* **2019**, *31* (8), 353−361.
(36) Duarte, M. L.; Ferreira, M. C.; Marvão, M. R.; Rocha, J. An Optimised Method to Determine the Degree of Acetylation of Chitin and Chitosan by FTIR Spectroscopy. *Int. J. Biol. Macromol.* **2002**, *31* (1−3), 1−8.
(37) Deboucha, W.; Leklou, N.; Khelidj, A.; Oudjit, M. N. Hydration Development of Mineral Additives Blended Cement Using Thermogravimetric Analysis (TGA): Methodology of Calculating the Degree of Hydration. *Constr Build Mater.* **2017**, *146*, 687−701.
(38) Loukili, A.; Khelidj, A.; Richard, P. Hydration Kinetics, Change of Relative Humidity, and Autogenous Shrinkage of Ultra-High-Strength Concrete. *Cem. Concr. Res.* **1999**, *29* (4), 577−584.
(39) Bhatty, J. I. Hydration versus Strength in a Portland Cement Developed from Domestic Mineral Wastes — a Comparative Study. *Thermochim. Acta* **1986**, *106*, 93−103.
(40) Kolani, B.; Buffo-Lacarrière, L.; Sellier, A.; Escadeillas, G.; Boutillon, L.; Linger, L. Hydration of Slag-Blended Cements. *Cem Concr Compos* **2012**, *34* (9), 1009−1018.
(41) Franus, W.; Panek, R.; Wdowin, M. Sem Investigation of Microstructures in Hydration Products of Portland Cement. *Springer Proceedings in Physics* **2015**, *164*, 105−112.
(42) Raheem, A. A.; Anifowose, M. A. Effect of Ash Fineness and Content on Consistency and Setting Time of RHA Blended Cement. *Mater. Today Proc.* **2023**, *86*, 18.
(43) Cruz Juarez, R. I.; Finnegan, S. The Environmental Impact of Cement Production in Europe: A Holistic Review of Existing EPDs. *Cleaner Environmental Systems* **2021**, *3*, No. 100053.
(44) Wernet, G.; Bauer, C.; Steubing, B.; Reinhard, J.; Moreno-Ruiz, E.; Weidema, B. The Ecoinvent Database Version 3 (Part I): Overview and Methodology. *International Journal of Life Cycle Assessment* **2016**, *21* (9), 1218−1230.
(45) Han, X.; Chang, H.; Wang, C.; Tai, J.; Karellas, S.; Yan, J.; Song, L.; Bi, Z. Tracking the Life-Cycle Greenhouse Gas Emissions of Municipal Solid Waste Incineration Power Plant: A Case Study in Shanghai. *J. Clean Prod* **2023**, *398*, No. 136635.
(46) Sevigné Itoiz, E.; Gasol, C. M.; Farreny, R.; Rieradevall, J.; Gabarrell, X. CO2ZW: Carbon Footprint Tool for Municipal Solid Waste Management for Policy Options in Europe. Inventory of Mediterranean Countries. *Energy Policy* **2013**, *56*, 623−632.
(47) Akbar, A.; Liew, K. M. Multicriteria Performance Evaluation of Fiber-Reinforced Cement Composites: An Environmental Perspective. *Compos B Eng.* **2021**, *218*, No. 108937.
(48) Li, X.; Lv, X.; Zhou, X.; Meng, W.; Bao, Y. Upcycling of Waste Concrete in Eco-Friendly Strain-Hardening Cementitious Composites: Mixture Design, Structural Performance, and Life-Cycle Assessment. *J. Clean Prod* **2022**, *330*, No. 129911.

https://doi.org/10.1021/acsomega.4c02040
ACS Omega 2024, 9, 24978−24986